

TRAJECTORY TRACKING BY DGPS-ODOMETRIC INTEGRATION FOR AUTONOMOUS VEHICLE WITH INDUSTRIAL APPLICATION

R. Da Forno,^a S. Badocco^a, A. Burlon^a

^a MDA, s.r.l., Viale Venezia 27, 31045, Motta di Livenza, Treviso, Italy
r.daforo@mda-net.com

KEY WORDS: DGPS, autonomous robot, navigation.

ABSTRACT

This paper presents an industrial application concerning the real time trajectory tracking of an autonomous heavy vehicle (up to 7000 kg) for material handling in industrial environment. Material handling in indoor environment has been successfully developed with navigation based on LIDAR system. In outdoor environment this solution is not reliable due to fog and rain disturbances. In this work we have develop the following modules: 1) trajectory planning with minimization of centrifugal acceleration, 2) DGPS-Odometric integration, 3) automatic calibration procedure.

The trajectory planning is based on the minimization of centrifugal acceleration in curved trajectory, obtained by connecting straight line with portion of cubic spiral. DGPS is based on hw Trimble in RTK, in order to real time control of the vehicle trajectory we need the integration of odometric localization based on wheel and steering angle measurement. DGPS information is used to set-up the odometric incremental localization. In this way the localization frequency is 33 Hz that allows the real time control. Automatic calibration is used in order: 1) to identify the transformation matrix between LIDAR ad topocentric DGPS frame of references; 2) to identify the position of the DGPS antenna in the vehicle frame of references.

The experimental measurements show an accuracy of ± 2 cm comparable with the LIDAR accuracy for indoor applications.

1. INTRODUCTION

Automated Guided Vehicle (AGVs) is a class of driverless ground vehicles. AGVs find application in industrial environment transporting raw material from warehouse to the shop floor, components form machine to machine and from process to process, all application in indoor environment.

In the recent years outdoor applications become very interesting due to the levitation of the cost of the industrial building. LIDAR solution for vehicle navigation, classical for indoor applications, for outdoor environment is not reliable due to fog rain, and snow disturbances. Similar conclusion can be stated considering navigation system based on vision system.

In this paper we propose a navigation system based on DGPS-RTK integrated with odometer in order to augment the position sampling rate. Trajectory generation is based on the minimization of centrifugal force, as proposed in (Cox, 1990).

In this work LIDAR system is used as reference measurement system in order to compare DGPS navigation and feedback control accuracy. An automated calibration procedure has been developed in order: 1) to identify the transformation matrix between LIDAR ad topocentric DGPS frame of references; 2) to identify the position of the DGPS antenna in the vehicle frame of references.

2. MATHEMATICAL MODEL

2.1 Vehicle model and control

The three wheeled vehicle model in based on classical approach (de Witt, 1996):

$$\begin{cases} \dot{x} = R\omega \cos \beta \cos \theta \\ \dot{y} = R\omega \cos \beta \sin \theta \\ \dot{\theta} = R\omega/L \sin \beta \end{cases} \quad (1)$$

For the symbols see Fig. 1, R is the front wheel radius.

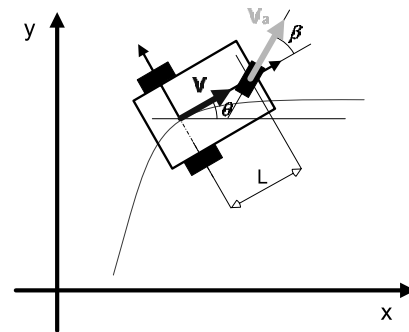


Figure 1. Vehicle kinematic scheme.

Given the nominal trajectory (x_0, y_0, θ_0) , by solving the inverse kinematic problem we can evaluate the front wheel angular velocity ω_0 and steering angle β_0 in order to achieve the nominal path. Introducing the tangent, normal, angular errors (e_t, e_n, e_θ) in the vehicle frame of reference we have:

$$e_t = (x_0 - x_m) \cos \theta_0 + (y_0 - y_m) \sin \theta_0 \quad (2)$$

$$e_n = -(x_0 - x_m) \sin \theta_0 + (y_0 - y_m) \cos \theta_0 \quad (3)$$

$$e_\theta = \theta_0 - \theta_m \quad (4)$$

where “m” means “measured”. Trajectory control is based on feedback and feedforward strategy:

$$\begin{pmatrix} u_\omega \\ u_\beta \end{pmatrix} = \begin{pmatrix} \omega_0 \\ \beta_0 \end{pmatrix} + \begin{matrix} \text{Feedforward} \\ \text{Feedback} \end{matrix} \begin{bmatrix} k_t & 0 & 0 \\ 0 & k_n & k_\theta \end{bmatrix} \begin{pmatrix} e_t \\ e_n \\ e_\theta \end{pmatrix} \quad (5)$$

where (k_t, k_n, k_θ) are the feedback gains. The odometer calculation are defined as follow:

$$\begin{cases} x_{k+1} = x_k + R \overbrace{\omega_k \Delta t}^{\Delta \alpha_k} \cos \beta_k \cos \theta_k \\ y_{k+1} = y_k + R \overbrace{\omega_k \Delta t}^{\Delta \alpha_k} \cos \beta_k \sin \theta_k \\ \theta_{k+1} = \theta_k + R \overbrace{\omega_k \Delta t}^{\Delta \alpha_k} / L \sin \beta_k \end{cases} \quad (6)$$

where $\Delta \alpha_k$ represents the incremental rotation of the front wheel between discrete time k and $k+1$, as measured by the encoder sensor, β_k is the steer angle measured at discrete time k , Δt represent the sampling time.

Odometer calculation is used to update the vehicle position within the DGPS sampling time (0.2 s, 5 Hz), odometer update frequency is 33 Hz in this work.

2.2 Trajectory planning

Trajectory is planned in order to minimize centrifugal acceleration in curved path, by minimizing the following functional (Cox, 1990):

$$\min_\gamma J(\gamma) = \min_\gamma \left(\int_0^l [\dot{\theta}(\lambda)]^2 d\lambda \right) \quad (7)$$

where γ is the oriented curve, θ in the vehicle attitude and λ is the curvilinear coordinate. Solution of (7) is a cubic polynomial in λ :

$$\theta(\lambda) = \frac{1}{6} A \lambda^3 + \frac{1}{2} B \lambda^2 + C \lambda + D \quad (8)$$

In Fig. 2 is shown an example of curve obtained from solution of (7), it is evident the continuity of the centripetal acceleration.

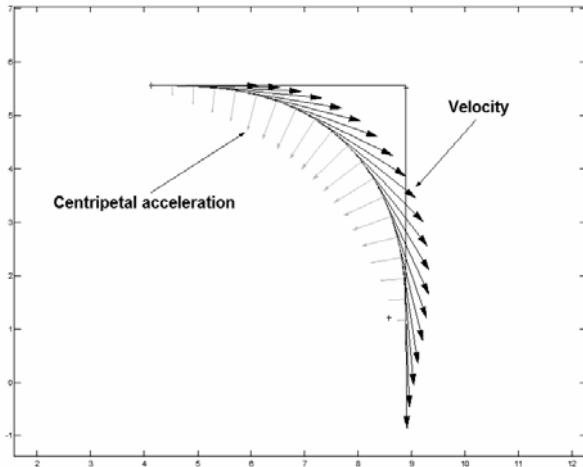


Figure 2. Example of curve obtained from solution of (7).

3. CALIBRATION

3.1 Topocentric calibration

In order to have a reference measurement system we have used an NDC LIDAR, while DGPS-Odometer is used to the real-time control of the vehicle trajectory.

In this work the term “topocentric calibration” means the determination of the transformation matrix between NDC frame of reference (f.o.r) and the local topocentric f.o.r.. In order to solve this problem we start with a straight line trajectory, with start point and slope known in both f.o.r.. Closure equation can be stated as:

$$\begin{matrix} \text{From DGPS} \\ \overleftarrow{N}T \\ \text{Unknown} \end{matrix} \begin{matrix} \overleftarrow{L}T \\ \overleftarrow{V}T \end{matrix} = \begin{matrix} \overleftarrow{N}T \\ \text{From NDC} \end{matrix} \quad (9)$$

where $\begin{matrix} B \\ A \end{matrix}T$, is the transformation matrix from f.o.r. A to B. In (9) V, L, N are, respectively, vehicle, local topographic and NDC f.o.r.. Solving (9) we obtain easily:

$$\begin{matrix} N \\ L \end{matrix}T = \begin{matrix} N \\ V \end{matrix}T \left(\begin{matrix} L \\ V \end{matrix}T \right)^{-1} \quad (10)$$

3.2 DGPS antennas calibration

The localization of the DGPS antennas can be defined with approximation with respect to the vehicle frame of reference, in order to enhance the accuracy of the trajectory tracking it is necessary to calibrate the position of the antennas. In Fig. 3 is shown a scheme of the vehicle with antenna number 1. The origin of the frame of reference named “1” represents the antenna position.

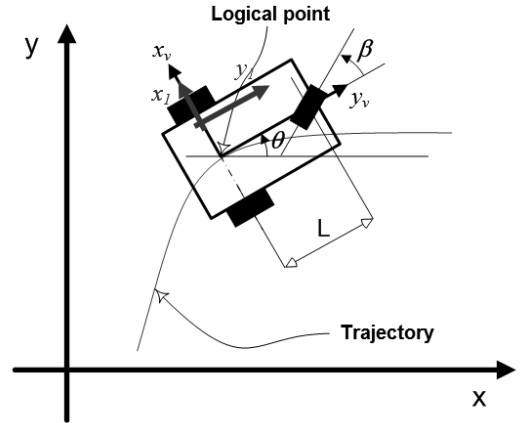


Figure 3. Scheme of the DGPS antenna position.

The relationship between f.o.r. 1 and vehicle f.o.r. V with respect to the inertial f.o.r. I can be stated as:

$$\begin{matrix} I \\ 1 \end{matrix}T \begin{matrix} 1 \\ V \end{matrix}T = \begin{matrix} I \\ V \end{matrix}T \quad (11)$$

In order to apply Kalman filter we need to define the measurement equation, this can be explained by rewriting (11) as follow:

$$\begin{matrix} \text{from DGPS} \\ \overleftarrow{I}T \\ \text{From vehicle dynamics} \end{matrix} = \begin{matrix} \overleftarrow{I}T \\ \overleftarrow{V}T \end{matrix} \left[\begin{matrix} \text{Unknown, depend on antenna position in V f.o.r.} \\ \overleftarrow{V}T \end{matrix} \right]^{-1} \quad (12)$$

Matrix ${}^i_v T$ depend on the vehicle state:

$${}^i_v T = \begin{bmatrix} \cos(\theta) & -\sin(\theta) & 0 & x \\ \sin(\theta) & \cos(\theta) & 0 & y \\ 0 & 0 & 1 & 0 \\ 0 & 0 & 0 & 1 \end{bmatrix} \quad (13)$$

while ${}^i_v T$ depend on the position of the antenna with respect to the vehicle f.o.r.:

$${}^i_v T = 0 \begin{bmatrix} 1 & 0 & 0 & p_x \\ 0 & 1 & 0 & p_y \\ 0 & 0 & 1 & 0 \\ 0 & 0 & 0 & 1 \end{bmatrix} \quad (14)$$

where p_x, p_y are the (unknown) coordinate of the antenna with respect to the vehicle f.o.r.. Summarizing, state equation is:

$$\begin{cases} \dot{x} = R\omega \cos\beta \cos\theta \\ \dot{y} = R\omega \cos\beta \sin\theta \\ \dot{\theta} = R\omega/L \sin\beta \\ \dot{p}_x = 0 \\ \dot{p}_y = 0 \end{cases} \quad (15)$$

measurement equation becomes:

$$z = {}^i_v T [{}^i_v T(p_x, p_y)]^{-1} \quad (16)$$

An example of calibration results are shown in Fig. 4 and 5.

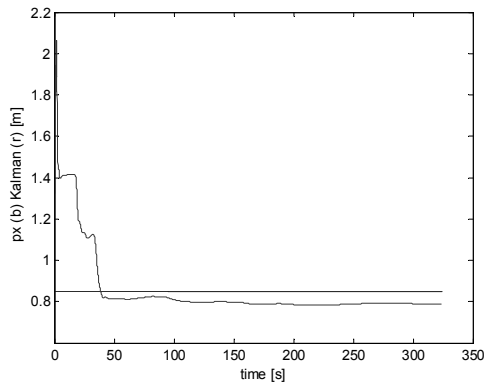


Figure 4. Calibration result for p_x .

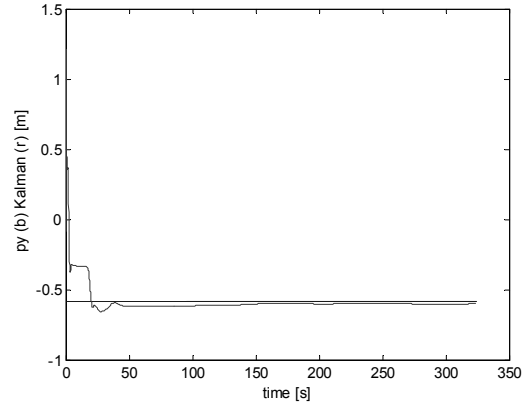


Figure 5. Calibration result for p_y .

Horizontal lines represent nominal value (from CAD model).

4. RESULTS

Solid model of the vehicle is shown in Fig. 6, experimental set-up is shown in Fig. 7.

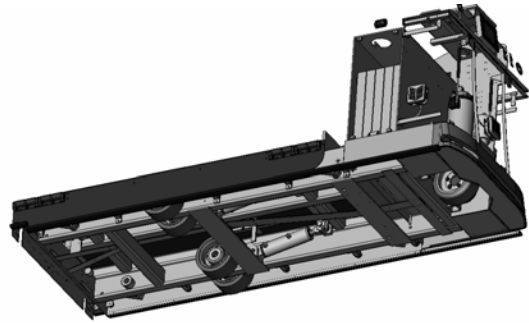


Figure 6. Vehicle solid model.

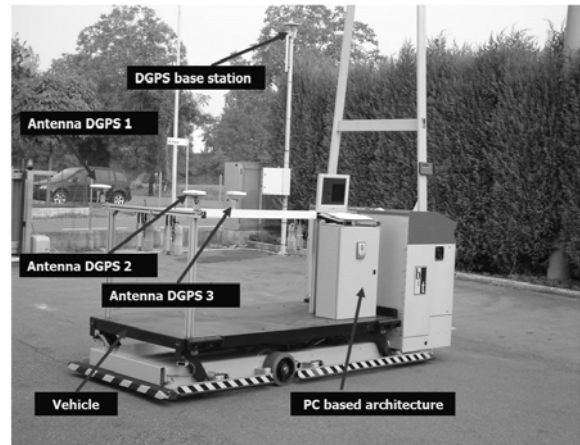


Figure 7. Experimental set-up.

In Fig. 8 is shown a typical time history of tracking error.

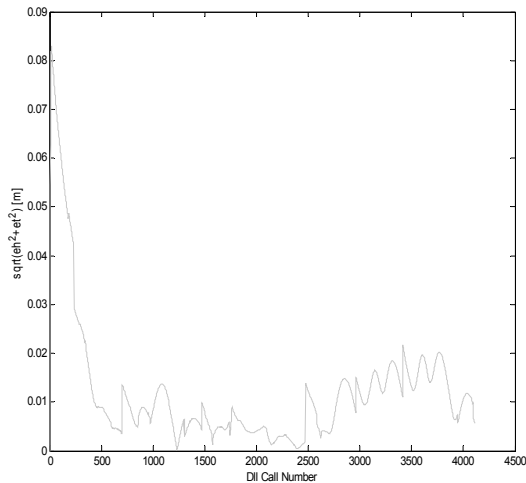


Figure 8. Experimental result: tracking error (in abscissa the discrete time, sampling rate 33 Hz).

In Fig. 9 and 10 is shown, respectively, the wheel at the start and at the end of the trajectory.



Figure 9. Rear left wheel at the start of the trajectory.



Figure 10. Rear left wheel at the end of the trajectory.

Positioning accuracy is ± 2 cm. Observe that the terrain is asphalt not perfectly flat.

5. CONCLUSIONS

In this paper has been analyzed an industrial application concerning the real time trajectory tracking of an autonomous heavy vehicle (up to 7000 kg) for material handling in outdoor industrial environment. Vehicle position measurement is based

on DGPS-RTK architecture, integrated with odometer update between DGPS sampling. Tracking accuracy obtained with experimental test is ± 2 cm comparable with the LIDAR based control strategy accuracy for indoor applications.

6. REFERENCES

- Cox, I., J., et al, *Autonomous Robot Vehicles*, 1990. Springer, Amsterdam, pp. 62-67.
- de Wit, C., C., et al, *Theory of robot control*, 1996. Springer, Amsterdam, Chap. 7.